Journal of Directed Energy, **1**, Winter 2006, 293–308

Thermal Energy Storage for Solid-State Laser Weapons Systems

C. B. Baxi*

General Atomics, 3550 General Atomics Court, San Diego, California 92121

and

T. Knowles

Energy Science Laboratories, Inc., 6988 Nancy Ridge Drive, San Diego, California 92121

The challenge to high-power solid-state laser (SSL) heat rejection is the very high heat loads during lasing. A thermal energy storage (TES) system capable of rapid heat absorption followed by heat rejection over a longer period can reduce the thermal management system size by over a factor of 10. The most compact system approaches to thermal storage use phase change materials (PCMs) such as ice or paraffin. Because of use of latent heat of fusion of these materials, a large amount of energy can be stored in a small mass of the storage material. The major drawback with this approach is the relatively low thermal conductivity of PCMs (ice at 1.9 and paraffin at 0.15 W/m-K compared to copper at 386 W/m-K). A new PCM system design approach is proposed that uses a "carbon fiber composite" material manufactured by Energy Science Laboratories, Inc. (ESLI), which dramatically increases the effective thermal conductivity of the PCM. The material consists of high conductivity carbon fibers, 2–5 mm long, bonded to a thin, flexible metal substrate. Water or paraffin is infiltrated into the carbon fiber structure, which can be constructed as circular tubes or flat plates. A high-heat-flux low-weight (HHF-LW) thermal storage system would consist of a number of plates in a heat exchanger configuration. The fluid used to cool the laser components is on one side of the heat transfer surface, and the recharge fluid from the chiller system is on the other side. The PCM material is "sandwiched" in between. The achievable value of k_{eff} (effective thermal conductivity) for the proposed HHF-LW depends on the density of fibers and the type of fiber used. With carbon fibers of thermal conductivity 1,100 W/m-K, a k_{eff} of ~100 W/m-K could reasonably be achieved. Preliminary analysis indicates that a k_{eff} of 60–80 W/m-K results in an optimum weight reduction in a TES system. A compact high-power thermal storage system using this technology can be fabricated to reduce the weight of the heat rejection system for SSHCL (solid-state heat capacity laser) by 90%. The estimated weight of the TES for 100 kW SSHCL is 180 kg.

KEYWORDS: Lasers, Thermal storage

Received May 4, 2004; revision received January 18, 2006.

*Corresponding author; e-mail: Chandrakant.Baxi@gat.com.

Nomenclature

A	area
Cp	specific heat of the coolant
Dh	hydraulic diameter
h	heat transfer cofficient
k	thermal conductivity
L	length of the heat exchanger
M	mass flow rate
Qs	total energy to be stored
Q''	energy flux to be stored
T	time
U	overall heat transfer coefficient, $1/(1/h + \delta/k_s + x/k_f)$
V	velocity of flow
W	width of the channel
X	phase charge material (PCM) thickness
x	instantaneous thickness of the melt layer
y	distance from the entrance
δ	wall thickness
λ	latent heat of the PCM
ρ	density of the coolant
ρ'	density of the PCM
τ	time in which the energy must be stored

Subscripts

f	phase change material
in	inlet
s	solid wall

1. Introduction

The thermal management system (TMS) will typically constitute 50% or more of the total weight of a high-power laser weapon system. Therefore, technologies that can reduce the weight of the TMS will have a large impact on the overall compactness and, therefore, extend the utility of the weapon system to a wider variety of platforms.

The large TMS weight fraction is due, in part, to the large thermal reject power. For example, a 100-kW-average-power solid-state laser (SSL) that has a 10% overall efficiency will have a thermal reject power of 900 kW during the lasing period. Key SSL heat transfer interfaces such as diode coolers and gain media surfaces typically must be maintained at (or reduced to) ~25°C. The maximum external environment temperature is typically ~35°C for airborne platforms and more than 50°C for ground-based systems. Thus, a very large chiller weight would be required if heat were rejected as fast as it were generated (Fig. 1). Figure 2 shows that if the SSL weapon heat were rejected at the rate at which it was produced, the resulting thermal management system size (~5,000 kg) would make SSLs impractical for mobile weapon system application. On the other hand, a thermal storage system, capable of rapid heat absorption followed by heat rejection over a longer period, can reduce the thermal management system size by a factor of 10 (e.g., ~500 kg).

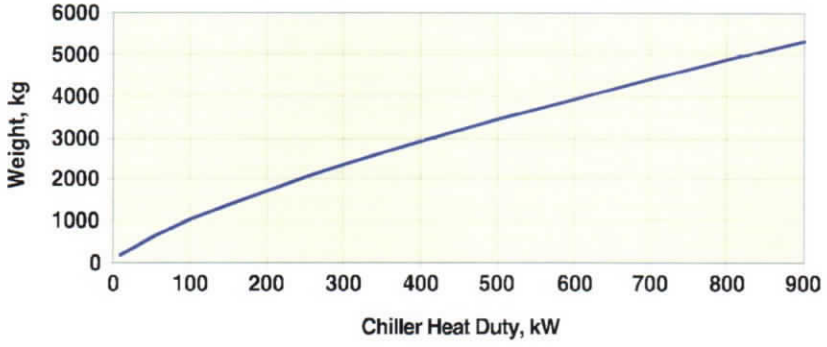

Fig. 1. Chiller heat duty vs. weight.

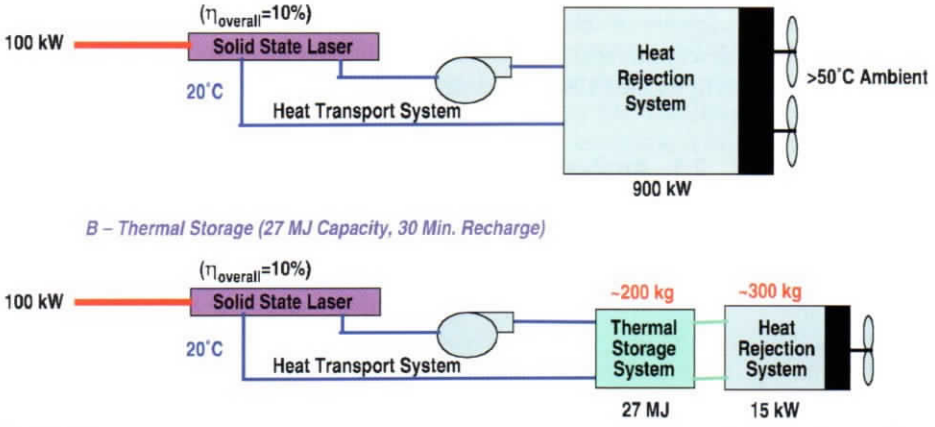

Fig. 2. Thermal storage system reduces SSL thermal management weight by factor of 10. If stainless steel is used as a material for the TES, the mass will be somewhat higher.

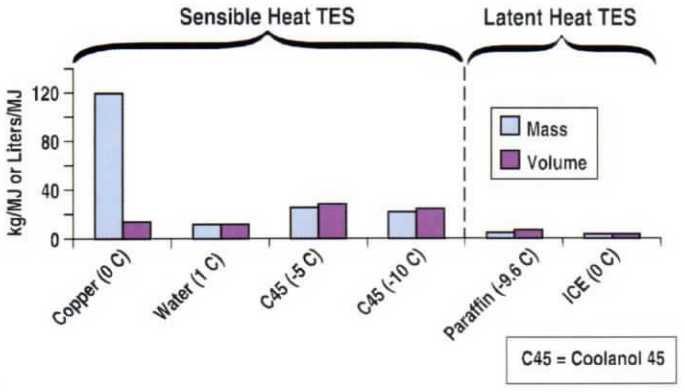

Fig. 3. Use of latent heat of PCMs reduces the weight of TES.

The simplest material for thermal storage is a metal such as copper with sensible heat used as a means to store energy. However, the weight required of the TES can be significantly reduced if the latent heat of phase change is used for thermal storage. Figure 3 shows the mass and volume required to store a mega joule of waste heat rejected at 20°C.

The major drawback with conventional thermal storage technologies[1–3,5] is associated with the low thermal conductivity of the phase change materials (PCMs) such as ice and paraffin (1.9 and 0.15 W/m-K, respectively, compared to that of copper at 386 W/m-K). This results in low heat input rates. Thus, in order to accommodate the high heat flux (HHF) associated with SSL weapon systems, conventional PCM systems require large heat transfer surface areas. This is the reason for the need to develop HHF PCMs. This translates into a smaller heat transfer surface, which can greatly reduce the weight reduction advantages of the thermal storage approach.

2. Analytical Development

In the TES under consideration, the rejected heat energy from the SSL is stored in the TES in a short time (30 s) relative to the time for final rejection to the environment (30 min). These times are based on the capacity of the electrical battery and the time required to recharge. The rate of energy delivery storage (i.e., required rate of melting the PCM) and the equivalent thermal conductivity of the PCM determine the heat transfer area.

2.1. Analysis model

As will be confirmed by the analysis, a key parameter in the development of a low-weight, high-power TES system is the high *effective* thermal conductivity of the PCM. Energy Science Laboratory, Inc., has developed a composite material by combining high-thermal-conductivity carbon fibers ($k \sim 1100$ W/m-K) with PCMs. Because of the very high thermal conductivity and low density (2.2 g/cc) of the carbon fibers, even a 10% volume fraction of the carbon fibers provides an effective thermal conductivity equal to 50% of that of a high conductivity metal like aluminum without a significant weight penalty. This type of PCM is called a phase change composite (PCC) material. In the following discussion, the effective thermal conductivity is the equivalent thermal conductivity of such a material.

Figure 4 shows a PCM at the phase change temperature T_f, which is receiving rejected heat at a temperature of T and a heat transfer coefficient of h. At time 0, the PCM is in a frozen state.

At the solid-liquid interface in Fig. 4, the amount of melting per unit time is equal to the heat transfer:

$$\rho' \lambda \frac{\mathrm{d}x}{\mathrm{d}t} \sim U(T - T_f). \tag{1}$$

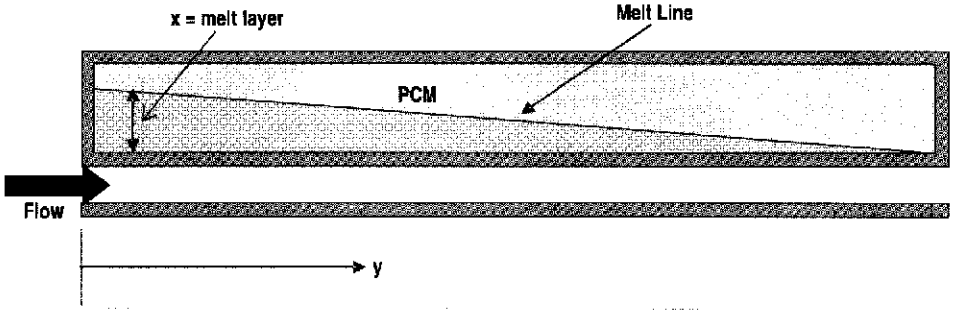

Fig. 4. Model of the PCM system.

The overall heat transfer coefficient U is the result of the external heat transfer coefficient h, the thermal resistance of the wall δ/k_s, and the thermal resistance of the molten layer x/k_f:

$$U = 1/(1/h + \delta/k_s + x/k_f). \tag{2}$$

Equation (1) can be integrated if one assumes that the coolant temperature does not change significantly from inlet to outlet and is equal to T. Thus, the required maximum useful thickness of the PCM, x, for storage time τ is

$$x = \sqrt{\frac{2k_f(T - T_f)\tau}{\rho'\lambda} + \left(\frac{k_f}{h} + \frac{\delta k_f}{k_s}\right)^2} - \left\{\frac{k_f}{h} + \frac{k_f\delta}{k_s}\right\}. \tag{3}$$

The total amount of energy flux stored is

$$Q'' = \rho'\lambda X. \tag{4}$$

The heat transfer area required to store energy, Q_s, can now be calculated as

$$A = Q_s/Q'', \tag{5}$$

$$A = Q_s/\rho'\lambda\sqrt{\frac{2k_f(T - T_f)\tau}{\rho'\lambda} + \left(\frac{k_f}{h} + \frac{\delta k_f}{k_s}\right)^2} - \left\{\frac{k_f}{h} + \frac{k_f\delta}{k_s}\right\}. \tag{6}$$

This derivation did not take into consideration the change in coolant temperature and change in melt layer thickness from inlet to outlet. This can be done by solving the transient energy equation for the coolant coupled with the PCM equation (3):

$$\frac{\partial T}{\partial y} = -(U/VW\rho Cp)(T - T_f) - 1/V\frac{\partial T}{\partial t}, \tag{7}$$

where V is the flow velocity and W is the channel width.

Equations (1) and (5) can be solved to determine the change in coolant temperature and thickness of the melt layer as a function of y and t. The total weight of the heat storage system will depend on the PCM weight, the weight of the heat exchanger, and flow distribution hardware. These can be easily calculated once the maximum value of melt layer (at $x = 0$) is determined.

2.2. Results of the analysis

A computer program was written to solve Eqs. (2) and (5) by an implicit numerical method. The coolant for the laser system was assumed to be water. The thermophysical properties of water were calculated as a function of temperature. The required input and output from the program are shown in Table 1.

The computer program was used to calculate the effects of different variables on the TES design.

Two critical parameters are the optimum thermal conductivity of the PCM and the outlet coolant temperature from the TES as a function of time. As seen in Fig. 5, the weight of the heat exchanger (HX) is reduced as the thermal conductivity of the PCM is increased due to a reduction in the heat transfer area. However, with a very high thermal conductivity, the volume fraction of the carbon fiber also increases and adds to the dead weight (i.e., it is a poor energy storage material). Hence, after a certain value of the effective thermal

Table 1. Input and output from the code

Input required to the code	Output from the code
Energy to be stored	Optimum thickness of the PCM
Time to store this energy in the TES system	Area of heat transfer required
Inlet temperature of the coolant	Pressure drop
Desired outlet temperature	Length required
Latent heat of the PCM	Mass of the HX
Effective thermal conductivity of the PCM	Coolant temperatures as a function of time and distance
Phase change temperature	Melt layer thickness as function of time and distance
Thermal conductivity of the fiber	
Density of the fiber	
Width of the coolant channel	
Thermal conductivity of the material of the heat exchanger	
Density of the material of the heat exchanger	
Thickness of the material of the heat exchanger	
Properties of the coolant	

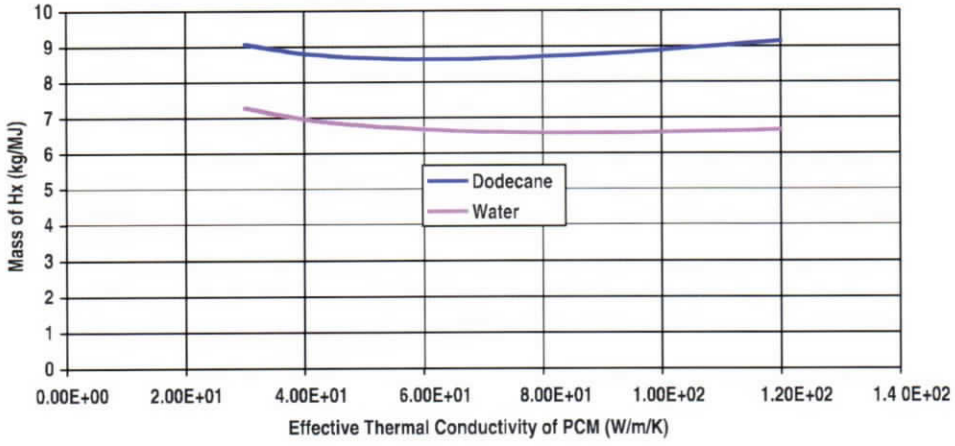

Fig. 5. Effect of effective thermal conductivity of PCM on kilograms/megajoules of the TES system for $T_{in} = 22^{\circ}C$ and $T_o = 20^{\circ}C$.

conductivity, the HX weight actually increases. A PCM effective thermal conductivity of 60–100 W/m-K seems to be an optimum for the parameters of interest.

The coolant outlet temperature must be uniform for use in the diodes because the temperature affects the diode optical output. The output temperature is fairly constant, as shown in Fig. 6. Using a bypass flow will make these temperatures even more uniform.

Table 2. Preliminary TES design for HCSSL (Cu-PCM-carbon fibers)

Variable	Paraffin	Ice	Variable	Paraffin	Ice
T_{in} (°C)	22	22	V (m/s)	4	4
T_o(°C)	20	20	ΔP (psia)	2	2
T_f(°C)	−9.6	0	PCM thickness (mm)	20	11
λ (kJ/kg)	225	334	A (m^2)	7.3	6.8
Material	Cu	Cu	L (m)	1.5	1.3
k_f (W/m-K)	60	60	MHX (kg/MJ)	8.6	6.7
W (mm)	2	2	M_{tot}	21	18

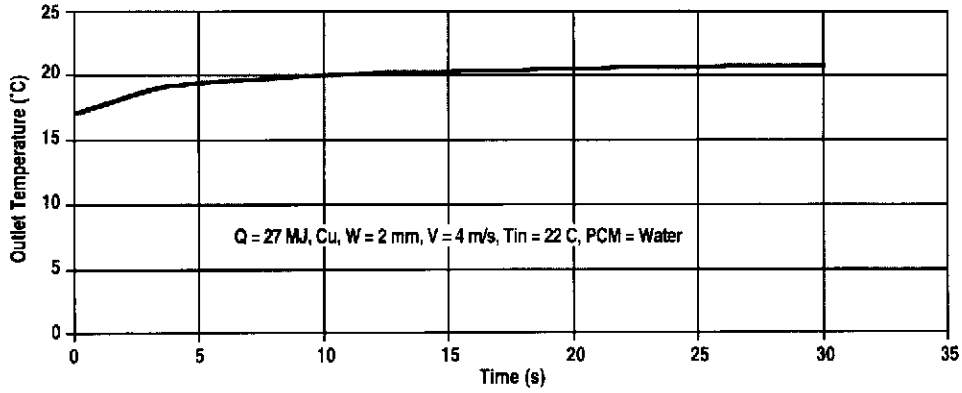

Fig. 6. Coolant outlet temperature as a function of time for $T_{in} = 22°C$ and $k_f = 60$ W/m/°C.

Several parametric studies such as effective flow channel width, required coolant outlet temperature, and effect of material of the HX weight were performed. This resulted in the selection of parameters for a preliminary design.

2.3. Preliminary design

A preliminary design was obtained for a heat capacity solid-state laser (HCSSL) system with a selected laser operation of 30 s. The recharge time for the battery system is selected as 30 min. Estimates show that for a laser device with a 100-kW output, the reject heat will be ~900 kW (assuming 10% total efficiency). The major portion of the reject heat comes from the diodes, which must be maintained at 20°C during operation. It was assumed that the cooling water enters the TES at 22°C and it is required to exit at 20°C, values typical of diode operation. The reject energy to store is 27 MJ. The resulting TES design is shown in Table 2 for two PCMs: dodecane and water. The larger weight for dodecane is due to a lower latent heat and a lower operating temperature. The lower freezing temperature (−9.8°C) of dodecane requires 10% higher chiller capacity than water (0°C) for the same heat load. The total (HX and chiller) weight requirement of 567 kg for dodecane is a factor of 8.8 improvement compared to a system without TES. If water is used as a PCM, the total weight will be less than 500 kg.

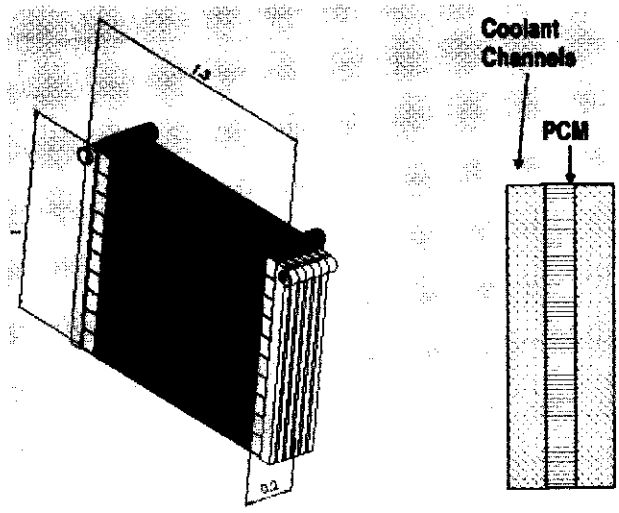

Fig. 7. Modular conceptual design of a TES for 27 MJ (dimensions in meters).

A sketch of a modular HX for this design is shown in Fig. 7. With this modular design, basically the same configuration can be used for a large range of heat loads.

3. Fabrication and Test of PCC-TES Articles

Several tests were performed to validate the heat exchanger performance critical in HEL TES applications.

3.1. Tubular PCM on pipe test article

Two flocked[4] copper U-tubes were fabricated with K1100 carbon fibers ($k = 1{,}100$ W/m-K), both having flocked fiber lengths of 3 mm and flock densities at the tube surface of about 0.8% by volume. Both tubes were 6-mm outer diameter and about 25 cm in length. The flocked and bare tubes were both bent into a U shape to allow immersion in a clear rectangular reservoir containing the liquid PCM. One flocked tube was tested and compared to a bare copper tube for freezing of both wax and water, using a cold liquid flowing through the tube.

Figure 8 shows the appearance of the setup with hexadecane frozen onto a carbon flocked copper U-tube, immediately following a run. The tube has been lifted out of the hexadecane reservoir.

Build-up rate data for the hexadecane runs for the bare vs. the flocked tube are shown in Fig. 9. The weight of hexadecane buildup was calculated from buoyancy measurements made manually every 10 s, which limits the time resolution of the method. It does clearly show the large improvement in the built rate of the flocked tube compared to the bare tube. The effect of the flock is even more dramatic than shown, since the manual weighing method could not capture fully the speed of the build rate. To the eye, the build appeared to happen in just a few seconds.

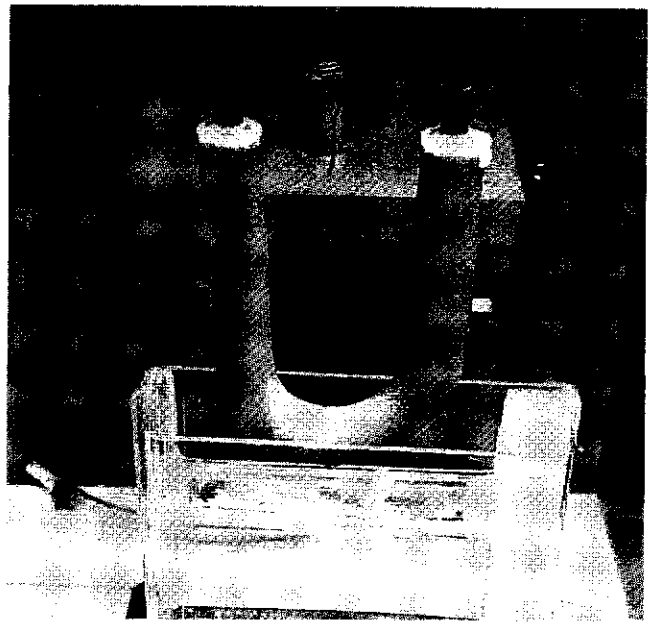

Fig. 8. Frozen hexadecane on carbon flocked copper U-tube.

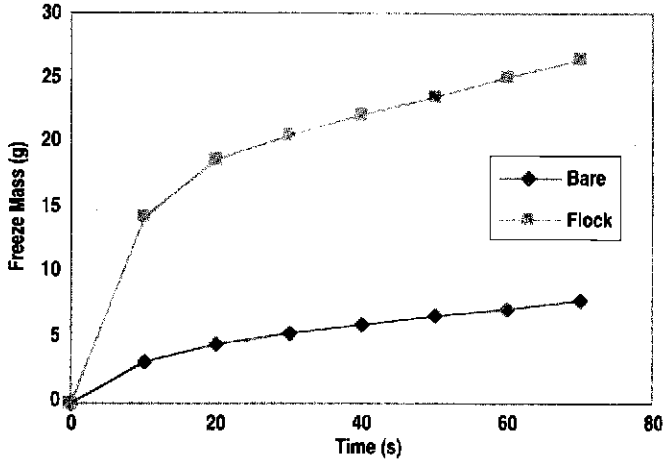

Fig. 9. Flocked vs. bare tube hexadecane build rate.

3.2. Cut-bar thermal conductivity test

The thermal interface between the carbon fiber and the exterior heat exchanger surface must be high quality to avoid being a high resistance component. A cut-bar thermal conductivity rig was used to measure the thermal resistance of two interfaces and a known length of known density carbon fibers. The cut-bar technique measures the temperature drop across the sample, which is placed between two rods of a material, the bar, with known thermal

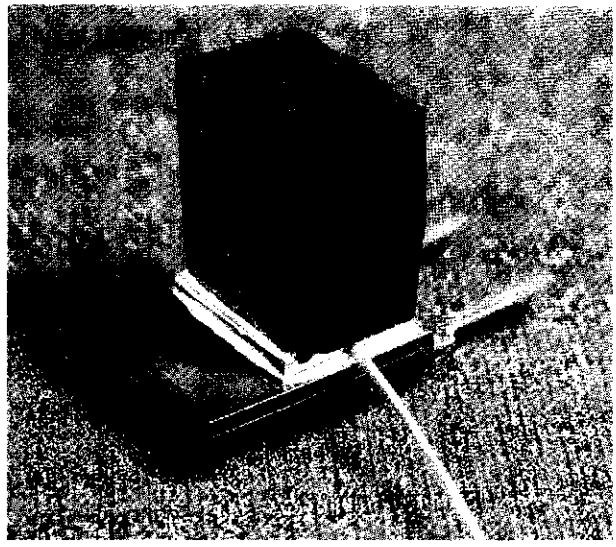

Fig. 10. High flux test article.

conductivity. The thermal gradient measured on both sides of the sample gives the heat flux in the rig.

The sample that gave the best interfacial conductivity was a 1-cm-high rectangular core of 10% K1100 fibers, bonded to the rods by using T7109 epoxy. The computed average thermal interfacial conductance was 33,250 W/m^2-K.

3.3. High flux test coupon

A small high flux test article (Fig. 10) was prepared and mounted on a Caddock MP9100 thin film resistance heater rated at 100 W when the case is heat sunk to 25°C. An aluminum bonding sheet was attached to the ceramic heater face to allow accurate measurement of the interface temperature. A fibercore made of 12.5% volume K1100 fibers (with an additional 2.5% of lower thermal conductivity carbon), 1.74 cm high with a base area of 1.65 cm^2, was attached to the aluminum plate using the standard EpoTek T7109 bonding technique. The maximum power applied to the sample was 30 W, which resulted in a flux of 18 W/cm^2.

Results from the thermal testing with 30 W of applied power are shown in Fig. 11. From the initial jump in the bottom temperature, the interfacial conductance was calculated as 42 kW/(K-m^2), using a previous run with 20 W of input power. The carbon fibercore conductivity was calculated from the slope of the bottom temperature as 133 W/(K-m), which is the expected theoretical value.

Five thermal cycles with ice were done with this test article using different power levels. The water was retained in the core by capillary action and then refrozen to ice for the next run.

This test demonstrated a flux level well above that required for the current thermal energy storage design, thus giving some margin for future performance increases.

4. Heat Exchanger Test Article

A small-scale test article with PCM was built using a Lytron CP25G02 high flux cold plate for convective heat transfer from the warm liquid to the PCC test article. The copper

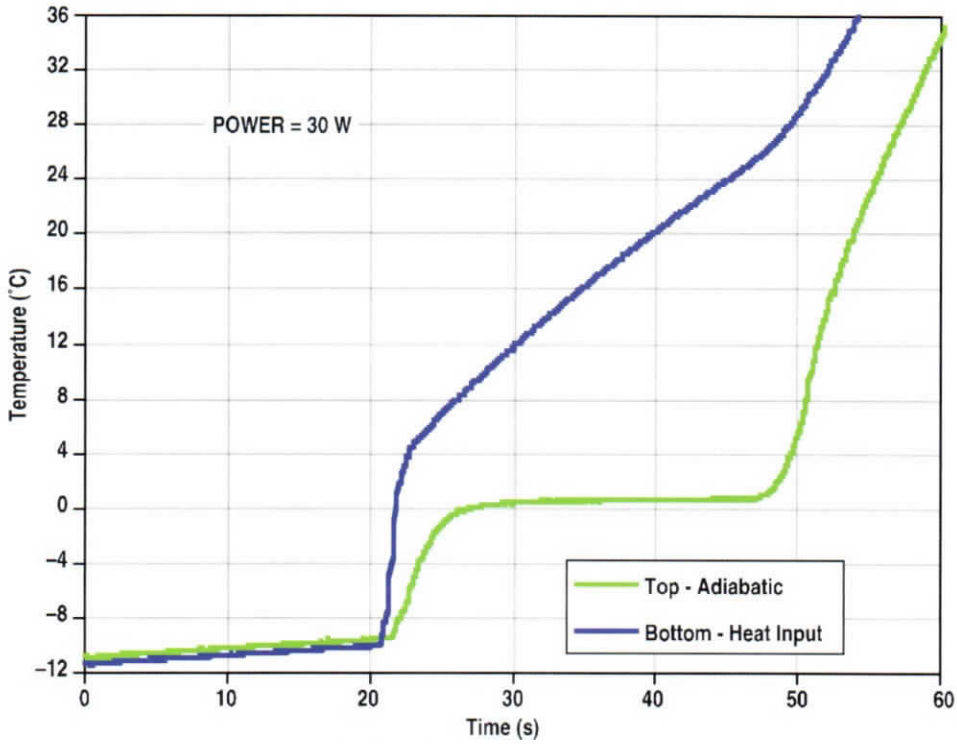

Fig. 11. High flux test results.

cold plate has fluid inlet and outlet connectors, with an internally structured heat exchanger surface measuring slightly over 2.5 × 5 cm. The PCC (phase change composite) was fabricated in an aluminum honeycomb, with an external frame made of a 0.020-in. C-channel 6061 aluminum. Thornel graphite fiber, with thermal conductivity $k = 1100$ W/m-K, was used at 10% volume fill fraction. The PCC and frame was bonded to the Lytron plate using EpoTek T7109 from Epoxy Technologies, which has BN conductivity filler. This article is shown in Fig. 12.

4.1. Experimental method

A data logging system was set up using National Instruments hardware and software. The software used was a Labview program to read thermocouple data, average, write to disk, and display values graphically on a monitor while running. An additional slower loop logged weight data from the coolant flow using a serial port.

The thermocouples used were all type E, which have a more sensitive response than other standard thermocouples. The thermocouples used were spot welded 36 AWG (~10-mil diameter) Teflon insulated wire. Thermocouple voltages were fed into the National Instruments SCXI-1000 multiplexing terminal and amplifier block, with temperature compensation for the reference junction. Calibration of the flow thermocouples was done with a straight through high-speed flow with room temperature water, which gives a negligible change in water temperature over a few inches of length.

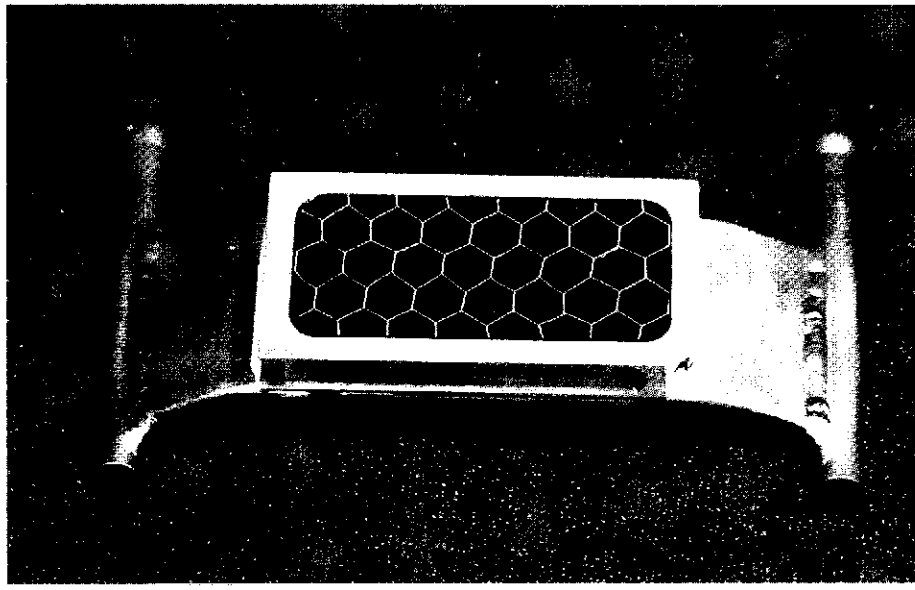

Fig. 12. PCC TES fiber core and frame mounted on Lytron cold plate.

Flow measurements were done using a King 2 gpm full-scale flow meter, with total accumulated flow measured by the data logging scale. Standard aneroid pressure gauges were used as appropriate to monitor gauge pressure along the liquid feed system. A pressurized barrel supplied pressurization for the flow with a liquid feed tube immersed in an internal bucket containing the water or water/ethylene glycol mixture being used to heat or cool the test article. Compressed shop air with an additional regulator was used to control the internal barrel pressure. Preheating or precooling of the supply line and flow meter was done by flowing the liquid through a bypass valve until the temperature at the bypass was effectively constant.

Commercial ethylene glycol was mixed with tap water to provide an appropriate margin of freezing point depression for the test being done. The high viscosity of the mixtures caused some early problems, which were dealt with by using lesser ethylene glycol concentrations and higher feed pressures.

4.2. Ice tests

For the initial two tests with water as the PCM, the plate was left open on the top. The three thermocouples used for measurement were loosely placed into the top of the water/fiber material by insertion through an insulating layer of foam. The plate was frozen by flowing a mixture of ethylene glycol and water through the test setup and monitoring the temperature. Freezing is easily seen on the screen plot of temperature as a leveling out of the fast downward trend. The temperature was taken well below freezing and then allowed to slowly warm back up to a few degrees below freezing, and then the high-speed flow for the test was started. Figure 13 shows one of the two ice melting runs. The cold plate inlet temperature is almost constant at just under 20°C, and the cold plate outlet temperature shows a steep rise toward the inlet as the thermally fast specific heat of the copper cold plate itself is warmed. The response of the backside of the ice is shown with the three thermocouple traces, with

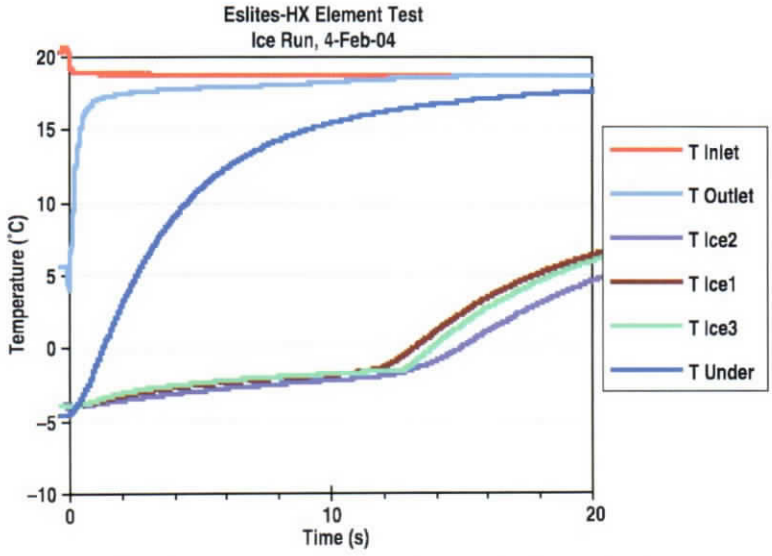

Fig. 13. Ice composite thermal test on Lytron cold plate.

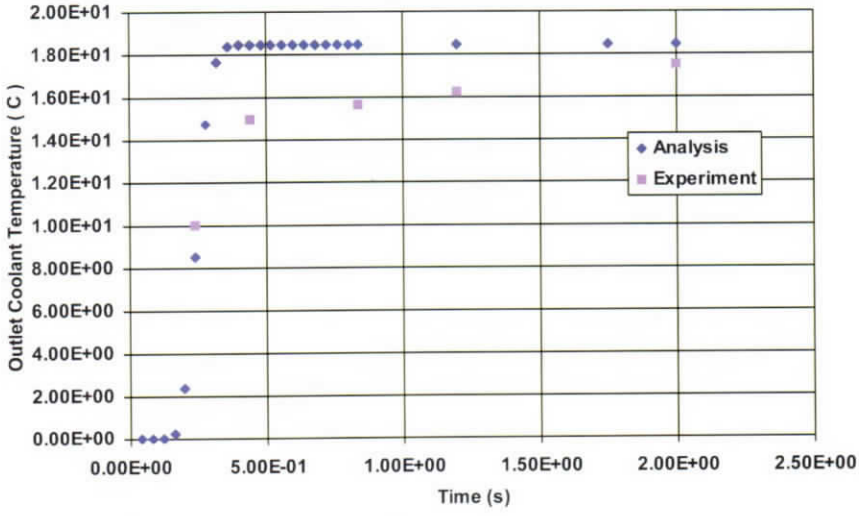

Fig. 14. Comparison of analysis and test results for ice test.

the end of melt-out shown by the sudden increase in slope at about 12 s, after the slowly rising trace during the melt-out. The backside temperatures all read about 2°C low, due to the competing influence of the ice at melting vs. the colder insulated leads still at several degrees below the melting point. The melt-out time is consistent with the measured liquid flow rate and temperature change, compared to the latent heat of the ice plus the sensible heat in the copper.

Comparison of analysis and test results shown in Fig. 13 is shown in Fig. 14. The slight difference in the results can be explained by rather larger thermal capacity of heat exchanger body in this experiment.

Fig. 15. PCC composite TES mounted to Lytron cold plate.

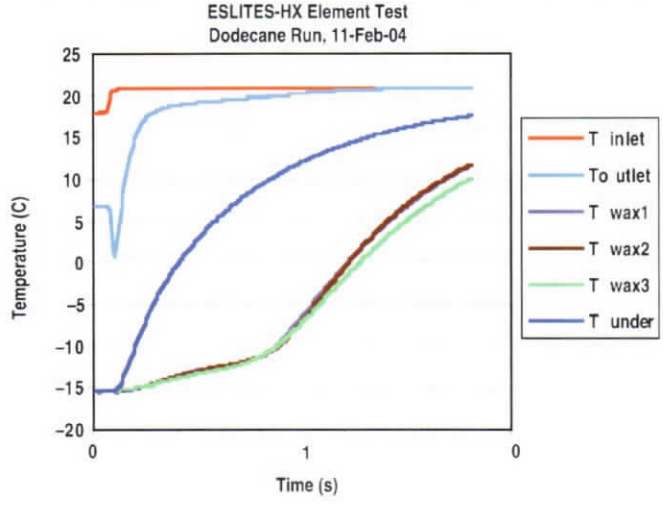

Fig. 16. Lytron cold plate thermal test with dodecane.

Upon completion of the ice tests, the core material was carefully rinsed to remove traces of small amounts of soap used as a surfactant and then dried. A close-out plate of aluminum was bonded on the top. The dodecane PCM was then added through a fill port, and the finished test article is shown in Fig. 15.

4.3. Dodecane tests

The thermal test data for one of the two runs with dodecane are shown in Fig. 16. The main differences from the ice runs are the faster speed of melt-out, due to higher temperature gradients and lower total latent heat, and the lower temperatures involved. The melting point of dodecane is −9.6°C.

4.4. Accuracy and error analysis of experiments

The liquid inlet and outlet thermocouples were checked against each other by placing the two thermocouples adjacent in the flow line and then running water at a relatively high

flow rate and logging the temperature. The measured offset between the two thermocouples, assuming that the water temperature was the same, was 0.07 K, with an approximate variation of the recorded temperatures of about 0.02 K about the mean.

The other thermocouples were not cross calibrated, due to the less critical nature of the temperatures they were measuring. The values of the three backside thermocouples measuring the melt-out were all within about 0.06 K of each other before the end of the melt-out plateau, which would be consistent with a relative accuracy of 0.1 K or better. These thermocouples were typically measuring temperature swings of several degrees.

A larger source of absolute temperature error was seen on the backside measurements, which were reading about 2 K lower than expected during the ice-melting plateau. We believe that this offset is consistent with the positioning of the thermocouple leads in an insulating layer above the base cold plate. The cold plate temperature was slowly brought up to about 5 K below the melting point, and then the high-flow-rate melt-out was begun. However, the leads in the thermocouple were still at an original starting temperature of several degrees Kelvin below the melt-out, resulting in a rough average temperature at the thermocouple between the PCM surface temperature and the lead temperature.

A quantitative check of the energy balance was done by integrating the temperature change of the water/antifreeze solution flowing through the Lytron test article, using the second run with ice. The total estimated sensible heat change, mainly in the copper plate, was 1,163 J, plus a total of 2,288 J in the phase change of 76.86 g of water. This is a total of 3,824 J. The total heat extracted from the plate was calculated from the temperature change as 3,787 J, which is about 101% of the total estimated thermal energy content. This energy balance provides good quantitative evidence of an overall energy balance in the measurement.

5. Conclusions

Based on analyses and experiments, the following conclusions were reached:

1. A LW TES design for high-power lasers is feasible. A performance index of <9 kg/MJ can be achieved. TES reduces weight, volume, and power requirements for solid-state laser weapons.

2. An analysis tool was developed to optimize the design of the TES system.

3. A high-k carbon fiber/phase-change material and high interface conductance was demonstrated to show that heat could rapidly be conducted into the PCM. The carbon fiber increases the PCM thermal conductivity to that of nearby aluminum.

4. The methods and materials developed are scalable for any paraffin.

5. Ice offers a 30% mass reduction in thermal storage and a ~15% reduction in mass of total heat rejection system.

6. A modular TES system applicable to all solid-state weapons can be designed with significant weight reduction.

References

[1]Dincer, I., and M. Rosen, *Thermal Energy Storage and Applications*, Wiley (2002).

[2]Pal, D., and Y.K. Joshi, J. Electronic Packaging **119**, 40 (1997).

[3]Pal, D., and Y.K. Joshi, Int. J. Heat Mass Transf. **44**, 375 (2001).

[4]U.S. Patents 6747093 and 6554945.

[5]Yanbing, K., J. Yi, and Z. Yinping, J. Solar Energy Eng. **121**, 185 (1999).

The Authors

Dr. Chandrakant Baxi is a 1971 graduate of the University of Michigan. He has been with General Atomics in San Diego for the past 33 years and is currently a Senior Technical Adviser in the Energy Division. He acts as an expert consultant on heat transfer to different divisions of General Atomics. He was responsible for all the aspects of *thermal design* of the experimental fusion machine, DIII–D Tokamak, located in San Diego. Dr. Baxi developed a method to analytically predict the thermal performance of hypervapotron, designed and tested a helium-cooled divertor design capable of thermal performance in excess of 10 MW/m^2, and recently developed a first-of-a-kind correlation for mist flow heat transfer for cooling laser slabs and electronic equipment. He suggested a conduction method to cool the laser slabs, which has been successfully implemented at GA. Dr. Baxi is an author/coauthor of more than 100 papers in the thermal sciences area, regularly reviews papers for technical journals, has a patent awarded to him, and has contributed to two published books. He was a guest editor for a special issue of *Fusion Technology on Thermal Hydraulics*.

Dr. Timothy Knowles is President of the Energy Sciences Laboratory in San Diego. He has conducted research in many novel heat transfer problems associated with energy storage on Small Business Innovative Contracts (SBIR). In this connection, he has collaborated with many U.S. government agencies including the DoD, DoE, and NASA. Some of the products designed and fabricated by Dr. Knowles have been installed on satellites and have performed as predicted.